Proceedings of ACIC 07
Advanced Composites in Construction
2nd – 4th April 2007, University of Bath, Bath, UK

INDIRECT ASSESSMENT OF THE CONTRIBUTION OF NSM CFRP LAMINATES FOR THE SHEAR STRENGTHENING OF RC BEAMS

Barros, J.A.O.[1], Oliveira, J.T[2]

[1,2] *Dep. of Civil Eng , School of Eng., Univ. of Minho, Azurém, 4810 058 Guimarães, Portugal*

Abstract: Near Surface Mounted (NSM) strengthening technique has received increasing attention within the scientific and technical communities due to the positive indicators that this technique can provide in terms of strengthening performance. The NSM is especially effective for the shear strengthening of RC beams due to the ease of its application and the possibility of installing the Fibre Reinforced Polymer (FRP) elements in the most appropriate locations for the optimization of their contribution in terms of shear resistance. Furthermore, the FRP elements are protected against acts of vandalism and do not change the geometric configuration of the strengthened components since they are installed into thin slits opened on the concrete cover. Although either circular or rectangular FRP bars are used, recent research shows that the latter (herein designated as laminates) are more effective and easier to install. Research carried out in the area of NSM for the shear strengthening of RC beams reveals that the percentage, inclination and spacing of FRP laminates have a considerable influence on the effectiveness of this technique. The percentage of existent internal stirrups, the relative position of stirrups and FRP laminates and concrete strength class are also important aspects for the performance of the NSM technique. To estimate the influence of these parameters, a new test setup is proposed and an experimental program has been planned. The test setup is similar to the indirect tensile test (Brazilian test). The experimental program consists of 27 cylindrical concrete specimens of 180 mm thickness and 600 mm diameter, grouped in series for evaluating the influence of the aforementioned parameters. The test setup is detailed, and the results of the first series are presented and discussed.

Keywords: *Near Surface Mounted, CFRP laminates, Shear strengthening, Debonding, Concrete, Critical Crack.*

1 Introduction

Near surface mounted (NSM) technique has proved to be a rather promising shear strengthening strategy for reinforced concrete (RC) beams [1, 2, 3]. This technique consists of fixing carbon fibre reinforced polymer (CFRP) laminates of $10\times1.4\ mm^2$ cross section, by epoxi adhesive, into thin slits opened on the lateral faces of the beams for strengthening purposes. Effectiveness of NSM technique can be measured by $I = \Delta F_{\max}^{Str} / F_{\max}^{\mathrm{Re}f}$ index, where $\Delta F_{\max}^{Str}$ is the beam maximum load increment provided by the CFRP strengthening configuration, and $F_{\max}^{\mathrm{Re}f}$ is the maximum load of the reference beam. Previous research has shown that larger *I* values were obtained in series of RC beams without internal steel stirrups than in RC beams with a certain percentage of steel stirrups, indicating the existence of a detrimental interactive effect between existent steel stirrups and CFRP laminate configurations [1, 2]. Furthermore, above a certain CFRP shear strengthening ratio (ρ_{fw}), NSM effectivenness seems to be dependent on concrete tensile strength, since a type of failure mode consisting of concrete cover separation occurred along the beam lateral surfaces [1, 2, 3], indicating that, above a certain limite of ρ_{fw}, no benefit can be obtained by the decrease of the spacing between laminates. Even for CFRP shear configurations of ρ_{fw} lower than this limit value, the laminates did not fail by pure debonding, as was assumed in the analytical model used for predicting NSM contribution for shear strengthening of RC beams [4]. To analyse the influence of the interference between existent steel stirrups and applied CFRP laminates, as well as the percentage of CFRP laminates in terms of the NSM shear strengthening efficacy, an experimental research was begun with round RC panels submitted to a stress configuration that aimed to reproduce the stress field at the critical region of RC beams failing in shear. The present work describes the test setup and presents and analyses results of the first series of tests of the experimental program.

[1] Associate Prof., Dep. of Civil Eng. barros@civil.uminho.pt
[2] Post-Doc Student, juliana@civil.uminho.pt

Table 1: Shear reinforcement and strengthening systems in the tested beams

Beam label	Age at beam test (days)	Shear reinforcement/strengthening in the smaller shear span (L_l)			
		Reinforcement/Strengthening	Quantity (ratios ρ_{sw} and ρ_{fw})	Spacing (mm)	Angle (º)
C_R	65	-	-	-	-
2S_R	61	Steel stirrups	2ϕ6 with two legs (0.10)	300	90
6S_R	62	Steel stirrups	6ϕ6 with two legs (0.24)	130	90
2S_3LV	72	Steel stirrups	2ϕ6 with two legs (0.10)	300	90
		CFRP laminates	2x3 laminates with 1.4x10 mm^2 (0.06)	267	90
2S_5LV	71	Steel stirrups	2ϕ6 with two legs (0.10)	300	90
		CFRP laminates	2x5 laminates with 1.4x10 mm^2 (0.10)	160	90
2S_8LV	70	Steel stirrups	2ϕ6 with two legs (0.10)	300	90
		CFRP laminates	2x8 laminates with 1.4x10 mm^2 (0.16)	100	90
2S_3LI45	66	Steel stirrups	2ϕ6 with two legs (0.10)	300	90
		CFRP laminates	2x3 laminates with 1.4x10 mm^2 (0.06)	367	45
2S_5LI45	64	Steel stirrups	2ϕ6 with two legs (0.10)	300	90
		CFRP laminates	2x5 laminates with 1.4x10 mm^2 (0.10)	220	45
2S_8LI45	68	Steel stirrups	2ϕ6 with two legs (0.10)	300	90
		CFRP laminates	2x8 laminates with 1.4x10 mm^2 (0.16)	138	45
2S_3LI60	71	Steel stirrups	2ϕ6 with two legs (0.10)	300	90
		CFRP laminates	2x3 laminates with 1.4x10 mm^2 (0.06)	325	60
2S_5LI60	67	Steel stirrups	2ϕ6 with two legs (0.10)	300	90
		CFRP laminates	2x5 laminates with 1.4x10 mm^2 (0.10)	195	60
2S_7LI60	68	Steel stirrups	2ϕ6 with two legs (0.10)	300	90
		CFRP laminates	2x7 laminates with 1.4x10 mm^2 (0.16)	139	60

$\rho_{sw} = \left[A_{sw}/(b_w d)\right] \times 100$ (stirrups ratio); ρ_{fw} (CFRP ratio - see equation 1)

2 Motivation

Fig. 1 represents a recent experimental program carried out in the context of assessing the influence of laminate inclination (angle β between CFRP fiber direction and beam axis), ρ_{fw} and interference between laminates and existent steel stirrups on the performance of the NSM technique for the shear strengthening of RC beams [2, 5]. The experimental program (see Table 1) was composed of one beam with no shear reinforcement (C-R beam); one beam with steel stirrups ϕ6@300mm (2S_R beam, with stirrups ratio ρ_{sw} = 0.10); one beam with steel stirrups ϕ6@130mm (6S_R beam, ρ_{fw} = 0.24); and nine beams of ϕ6@300mm with different CFRP strengthening arrangements on the L_l beam half-span (Fig. 2): three ρ_{fw} and, for each ρ_{fw} three different β (90º, 45º and 60º). The CFRP shear strengthening ratio ρ_{fw} was obtained from the Eq. (1):

$$\rho_{fw} = \frac{2 \cdot a_f \cdot b_f}{b_w \cdot s_f \cdot sen\ \beta} \times 100 \qquad (1)$$

where a_f = 1.4 mm and b_f = 10 mm are the laminate cross section dimensions; b_w = 180 mm is the beam web width; and s_f is the spacing between laminates. For the three series of beams with different laminate angles, the maximum ρ_{fw} in each series was evaluated to ensure that the beams presented a maximum load similar to the 6S_R reference beam, which was reinforced with the highest ρ_{sw}. In the evaluation of the maximum ρ_{fw}, it was assumed that CFRP works at a stress level corresponding to 5‰ strain, which is a compromise between the 4‰ value recommended by ACI for EBR [6], and the 5.9‰ value obtained in pullout bending tests on NSM laminates [7]. For the intermediate and minimum ρ_{fw}, the spacing s_f for 90º, 60º and 45º was evaluated to obtain a similar laminate contribution for each ρ_{fw}.

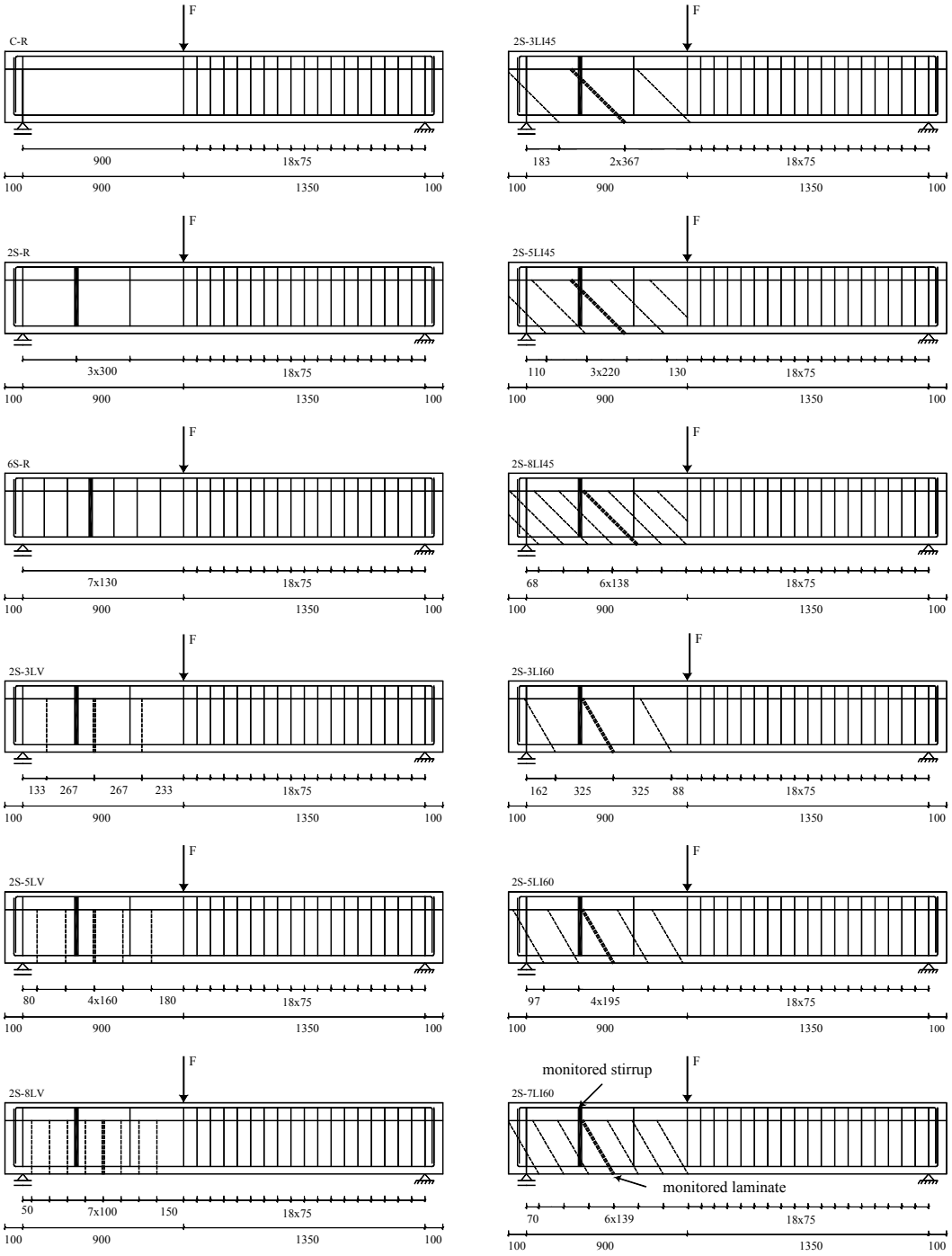

Figure 1: Tested beams: position of steel stirrups (thick line) and CFRP laminates (dashed line)

In Fig. 2 the laminates are distributed along the AB line, where A is the beam support at the "test side" and B is obtained assuming a load degradation of 45º.

Considering that the resisting shear force in the smaller beam shear-span *i.e.* $V_r = 0.6\ F_{\max}$ (see Fig. 2) is obtainable through adding the several contributions $V_r = V_c + V_s + V_f^{\exp}$ ascribed to the concrete, V_c, steel stirrups, V_s, and CFRP laminates, $V_f^{\exp}$, the latter of which was determined accordingly. The main results are included in Table 2. The properties of the materials, the detailed discussion of results and failure modes can be found elsewhere [2, 5]. The failure modes occurring in the beams indicated in Fig. 3 are analysed for the interest of the present work. From Table 2 it can be verified

that the $V_f^{\exp}$ value for the 2S_3LV beam was excessively low, since the contribution of the steel stirrups (V_s) in this beam was much lower than that in the 2S_R reference beam. In fact, by post-test inspections it was verified that in the 2S_R reference beam, the critical diagonal crack intersected two stirrups, while in the 2S_3LV beam two critical diagonal cracks formed, each one only crossed by one steel stirrup (see Fig. 3a and 3b). Moreover, per beam lateral surface, only one laminate crossed each critical diagonal crack and the laminate pulled out length did not exceed 80 mm. The NSM shear strengthening configuration of the 2S_3LI45 beam also provided a relatively low contribution for beam shear resistance. Two shear failure cracks were also formed, each one crossed by one steel stirrup, and the pulled out length of the intermediate laminate was 125 mm (see Fig. 3c).

Table 2: Summary of relevant results of the tested beams

Beam label	F_{max} (kN)	$\Delta F_{\max} / F_{\max}^{2S-R}$ (%)	F_{max} / F_{max}^{6S-R}	$V_f^{\exp}$ (kN)	$V_f^{\exp} / V_r^{2S-R}$ (%)
C_R	243	-	0.59	-	-
2S_R	315	0.0	0.77	-	-
6S_R	410	30.2	1.00	-	-
2S_3LV	316	0.3	0.77	0.6	0.3
2S_5LV	357	13.3	0.87	25.2	13.3
2S_8LV	396	25.7	0.97	48.6	25.7
2S_3LI45	328	4.1	0.80	7.8	4.1
2S_5LI45	384	21.9	0.94	41.4	21.9
2S_8LI45	382	21.3	0.93	40.2	21.3
2S_3LI60	374	18.7	0.91	35.4	18.7
2S_5LI60	392	24.4	0.96	46.2	24.4
2S_7LI60	406	28.9	0.99	54.6	28.9

The $V_f^{\exp}$ of the 2S_3LI60 beam was the highest one amongst the beams with the minimum ρ_{fw} due to the formation of only one shear failure crack that was crossed by two steel stirrups and one laminate with a pulled out length of 100 mm. When compared to the contribution provided by the laminates of the 2S_3LI45 beam, the higher contribution of the laminates in the 2S_3LI60 beam can be also attributed to the detrimental interference between laminates and existing steel stirrups. In fact, the steel stirrup closer to the left support of the 2S_3LI45 beam (see Fig. 3c) crossed the pulled out length of the laminate that effectively contributed to shear strengthening. This detrimental effect did not occur in the 2S_3LI60 beam. This highlights the importance of taking into account the possible interaction between existing steel stirrups and applied laminates. Fig. 3e and 3f show that, for the beams strengthened with the maximum ρ_{fw}, i.e., beams with smaller laminate spacing, two "concrete lateral walls" separated from the beam concrete core. This indicates that the concrete tensile strength plays an important role in limiting the contribution of these CFRP systems for the shear strengthening of RC beams.

To assess the influence of the interaction between laminates and existent steel stirrups in a T cross section RC beam as well as laminate spacing, in terms of NSM shear strengthening effectiveness using a relative low cost test setup, the hypothesised approach is schematically illustrated in Fig. 4. This effectiveness can be evaluated from the strain profile in the laminates during the specimen loading process, as well as the maximum strain that may be applied to the laminates. Furthermore, the influence of laminate inclination on NSM effectiveness can easily be assessed adopting this test setup.

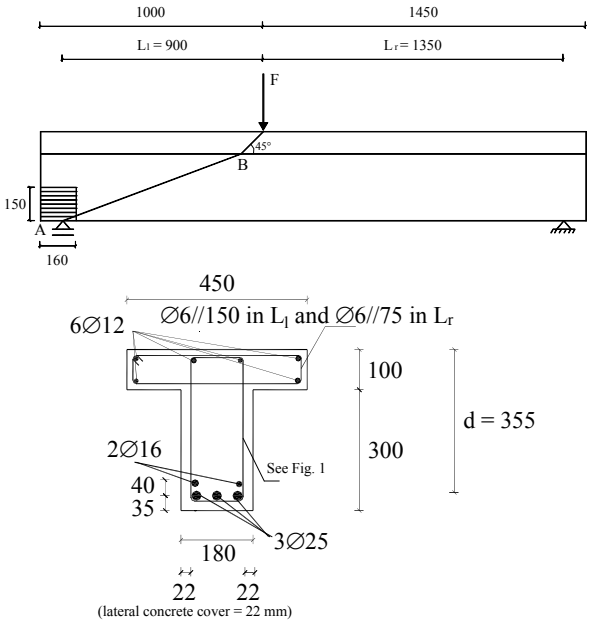

Figure 2: Beam prototype: geometry, steel reinforcements, loading and support conditions (dimensions in mm)

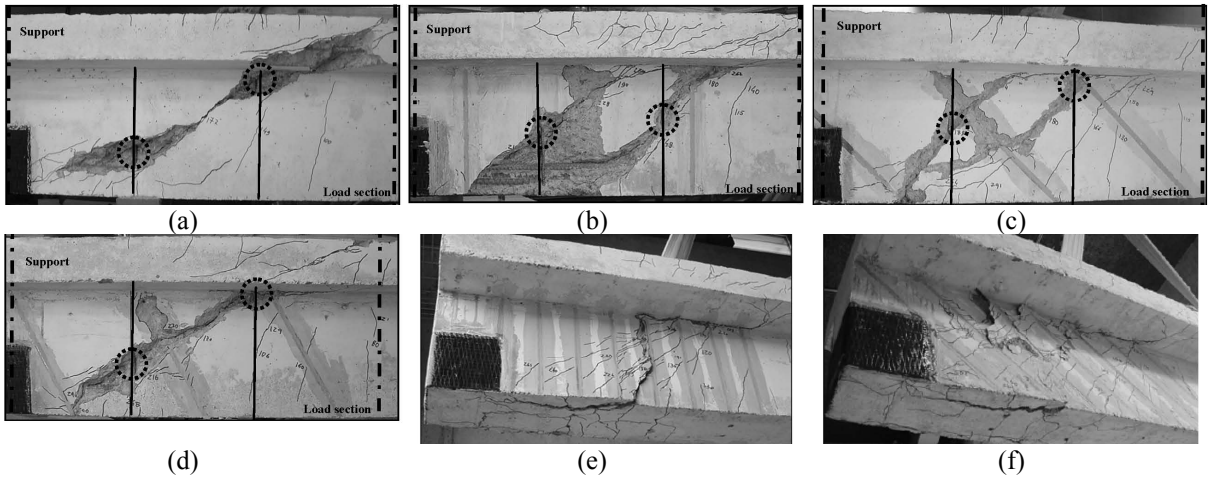

Figure 3: Some details of the failure zones of beams: (a) 2S_R; (b) 2S_3LV; (c) 2S_3LI45; (d) 2S_3LI60; (e) 2S_8LV;(f) 2S_8LI45

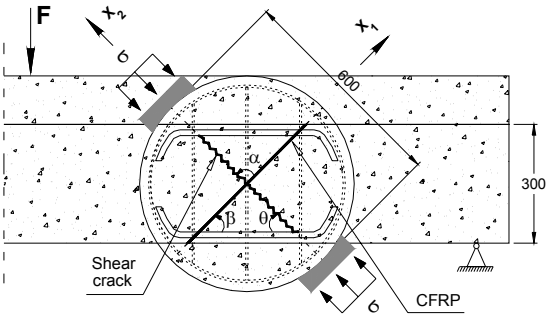

Figure 4: Idealization of a test setup for the capture of the phenomena in discussion (dimensions in mm)

3 Experimental Program

3.1 Series

Fig. 5 represents specimen characteristics of the first test series of the experimental program. The specimens have the same web beam thickness of the experimental program referred to in Section 2 (180 mm), and a diameter of 600 mm. L0S0 is the reference specimen, L4S0 has only CFRP laminates of distinct embedded lengths, L1S3, L2S3 ad L7S3 have three steel stirrups in the test zone, but with a distinct number of laminates, one, two and seven, respectively, per each face of the specimen. A specimen (L0S3) without laminates and with an arrangement of conventional steel bars equal to the ones of the last three specimens was also built but, due to mal-functioning of the test equipment, the results of this test were lost.

Fig. 6 represents details of the steel reinforcement to reproduce, as much as possible, the reinforcement arrangement of a T cross section beam. The steel stirrups were extended to the top part of the specimen to simulate the anchorage conditions found in a T beam where the stirrups embrace the top longitudinal reinforcement placed in the beam flange. To avoid undesirable premature failures, supplemental stirrups were placed in the bottom part of the specimen, outside the testing zone, and two steel bars of 6 mm diameter were positioned along the contour of the specimen.

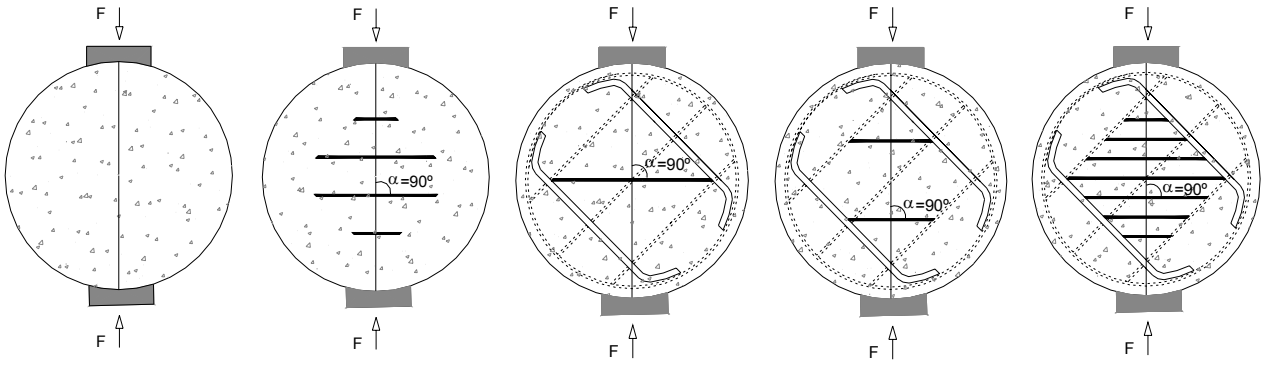

Figure 5: Specimens of the 1st series of the experimental program: a) L0S0; b) L4S0; c) L1S3; d) L2S3; e) L7S3 (the vertical line, coinciding with the vertical specimen symmetry plan, represents the loading plan)

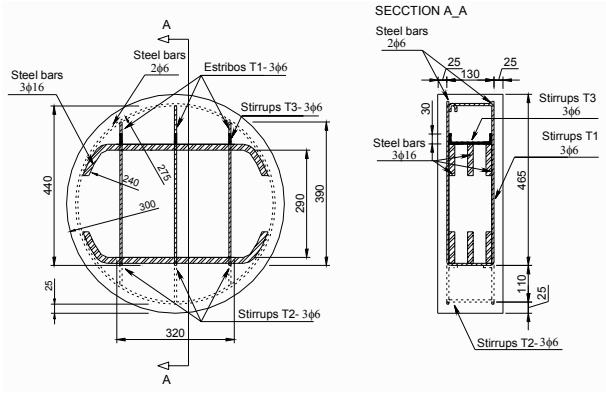

Figure 6: Arrangement of the conventional reinforcement (dimensions in mm)

3.2 Specimen Preparation and Strengthening Procedures

Each specimen was cast in two layers of similar thickness in order to assure good concrete compactness, without damaging the strain gauges installed in the steel stirrups. After casting, the specimen top surface was covered with wet burlap for 4 days. After this period, and up to the test age, which occurred at about 50 days, the specimens remained in the natural environmental conditions of the laboratory.

The CFRP strengthening system was applied by the following procedures: 1) using a diamond blade cutter, slits of about 5 mm width and 12 to 15 mm depth were cut on both faces of the specimen, according to the pre-defined arrangement for the laminates; 2) slits were cleaned by compressed air; 3) laminates were cleaned by acetone; 4) epoxy adhesive was prepared according to supplier recommendations; 5) slits were filled with the epoxy adhesive; 6) epoxy adhesive was applied on the faces of the laminates; and 7) laminates were introduced into the slits and epoxy adhesive in excess was removed.

3.3 Test Setup, Monitoring Strategy and Test Procedures

As Fig. 4 shows, in the present exploratory series of tests, the direction of the failure crack was assumed as making an angle of 45 degrees with the vertical existent steel stirrups of RC beams to be strengthened, which is supported by the available research [6, 8, 9]. To form this failure crack, using a servo-controlled machine of load carrying capacity of 2000 kN in compression and 200 kN in tension, the specimens were installed in the equipment in such a way that the vertical loading axis coincided with the direction of the failure crack to be formed (Fig. 7). To avoid excessive stress concentration in the specimen zones submitted to the influence of the machine loading platens, two intermediate steel supports, with a surface configuration adjustable to the geometry of the specimen, were interposed between these platens and the specimen (Fig. 7b).

Fig. 8 indicates the positions of the strain gauges glued on steel stirrups and on laminates of the tested specimens. On each face of the specimen, two LVDTs were placed, one to measure the vertical deformation and the other to measure the horizontal deformation (see Fig. 7b). The measuring length of both the vertical and horizontal LVDTs was 424 mm. An extra vertical LVDT was used to control the test at a displacement rate of 2μm/s. The applied force was measured from a load cell of 2000 kN capacity.

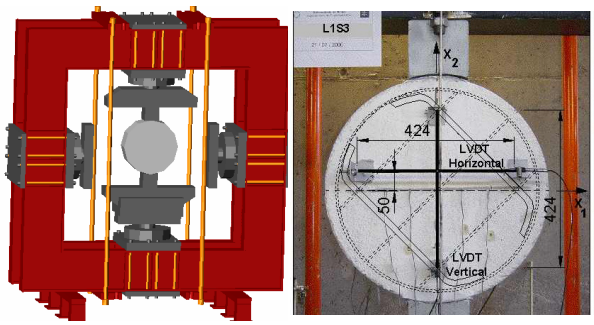

Figure 7: (a) Equipment and (b) test setup (dimensions in mm)

3.4 Material Properties

The compressive strength and Young's modulus of the concrete applied to manufacture the specimens were obtained at 28 days according to the RILEM recommendations [10]. The average of the results obtained in three cylinder specimens (150 mm diameter and 300 mm height) was 37 MPa for the compressive strength, and 30.3 GPa for the Young's modulus.

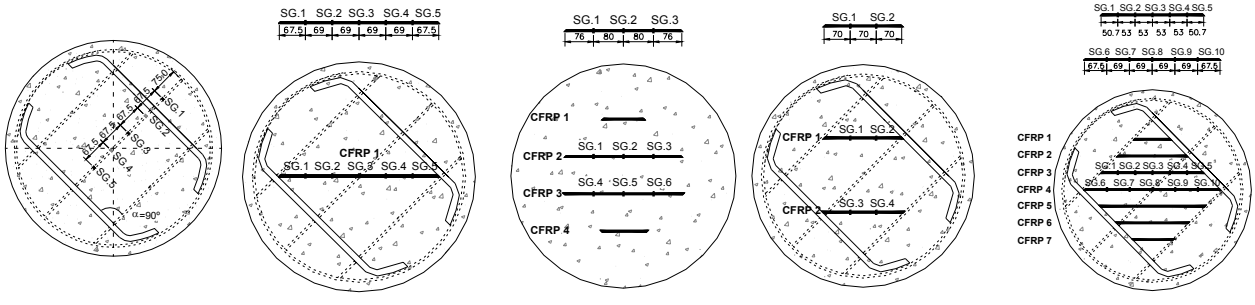

(a) (b) (c) (d) (e)

Figure 8: Strain gauges applied in the: (a) steel stirrups; (b, c, d, e) laminates (dimensions in mm)

To evaluate the tensile properties of the steel bars reinforcing the specimens, tensile tests were carried out according to the EN 10 002-1 recommendations [11]. Table 3 includes the main results.

The CFRP laminates were supplied by S&P Company, and had a cross section of 10×1.4 mm^2. Four tests were also carried out according to the ISO 527-5 recommendations [12], from which the following average values were obtained: tensile strength (f_{fu}) of 2879 MPa; elasticity modulus (E_f) of 156.1 GPa; and strain at peak stress (ε_{fu}) of 18.4‰.

From nine tensile tests with specimens of the epoxy adhesive used to fix the laminates to the concrete substrate, carried out according to Ref. [13] recommendations, an average tensile strength of 33.03 MPa (with a standard deviation of 2.81 MPa and a COV of 5.76%); an average modulus of elasticity of 7.47 GPa (with a standard deviation of 0.32 GPa and a COV of 4.28%); and an average ultimate strain of 4.83‰ (with a standard deviation of 0.57‰ and a COV of 11.8%) were obtained [14].

Table 3: Tensile properties of the steel reinforcement

Diameter (mm)	E_s * (GPa)	$\sigma_{y0.2\%}$ * (MPa)	$\varepsilon_{y0.2\%}$ * (‰)	σ_{max} * (MPa)
6	198.04 (2.11) [1.07%]	439.58 (7.30) [1.66%]	4.2 (0.02) [0.6%]	568.28 (7.01) [1.22%]
16	196.61 (17.81) [9.06%]	405.90 (2.98) [0.73%]	4.1 (0.14) [4.25%]	553.84 (5.70) [1.03%]

* Average value (standard deviation) [coefficient of variation]

3.5 Results and Discussion

Fig. 9 includes the relationships between the applied force and the strains measured by the LVDTs in both vertical and horizontal directions (negative values correspond to compressive strains). Each curve is the average of the displacement values recorded in the corresponding LVDTs placed on the front and rear faces of the specimen, divided by the LVDT measuring length (424 mm) to convert displacements into strain values. The main obtained results are included in Table 4, where F_{cr} is considered to be the load at the moment when crack formation was visible, and F_{max} is the maximum load. The crack pattern of the tested specimens is shown in Fig. 10. Analysing these figures, it can be observed that in the L0S0 specimen a vertical crack plane parallel to the loading plane was formed at about 570 kN. Due to circumferential tensile stresses developed near the contour of the specimen, some radial cracks were formed. Just after the formation of the main crack, a short load decay occurred, followed by a "hardening branch" of lower stiffness up to the peak load (751 kN), which occurred at an average specimen vertical deformation of 1.5 ‰. After peak load, the specimen entered a softening phase up to an axial specimen vertical deformation of about 5.4 ‰.

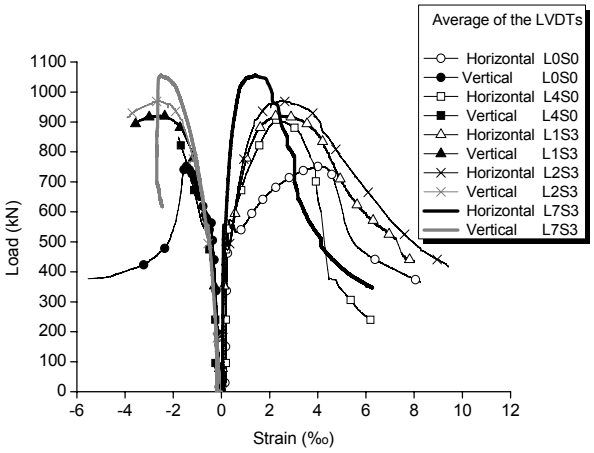

Figure 9: Force versus vertical and horizontal strains

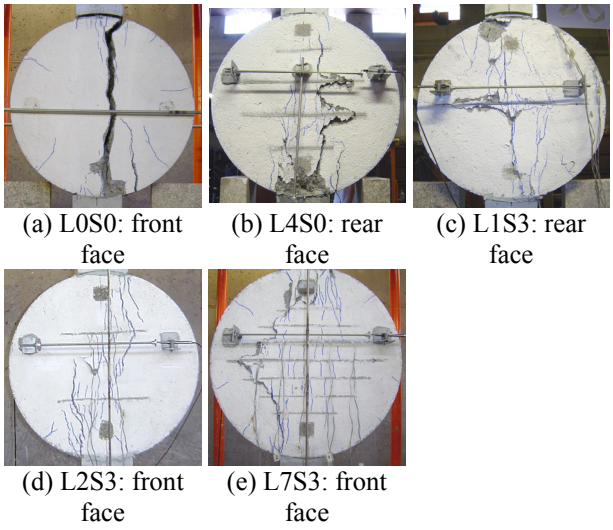

(a) L0S0: front face (b) L4S0: rear face (c) L1S3: rear face

(d) L2S3: front face (e) L7S3: front face

Figure 10: Crack patterns of specimens: a) L0S0; b) L4S0; c) L1S3; d) L2S3; e) L7S3

As expected, the influence of the laminates was only significant after crack formation. This was already verified in the T cross section RC beams, where the effectiveness of the CFRP laminates was only visible after the formation of the shear critical crack [2]. From the comparison of the F-ε of specimens strengthened with CFRP laminates, it is concluded that both the stiffness after crack formation and the specimen load carrying capacity (F_{max}) increased with the increment of the CFRP strengthening ratio,

$$\rho'_{fw} = A_f / (b_w \times h) = (n_f \times 2 \times 10 \times 1.4) / (180 \times 300 \times \sqrt{2}) \times 100 \quad (2)$$

where $h=300\times\sqrt{2}$ mm is the depth of the test zone, which coincides with the measuring length of the vertical LVDT (see Fig. 7b) and n_f is the number of laminates crossing the loading plane. However, as Fig. 11 shows, the increase of the F_{max} seems to decrease with the increase of ρ'_{fw}, which is justified

by the type of failure modes that occurred. In fact, Figs. 10c and 10d show that for the cases of large spacing between laminates, each laminate contributes to the crack opening arrestment, in its plenitude, while in the L4S0 and L7S3, primarily in this last one, the group effect is very visible due to the mutual interference between consecutive laminates. In L7S3 a concrete layer that includes the CFRP laminates separated from the specimen concrete core. It is also interesting to note that, even for large distance of laminates, pure debonding did not occur, since some concrete volume is always attached to the pulled-out length of the laminates. The decay of CFRP strengthening efficacy with the increase of ρ'_{fw} is also visible from the analysis of the maximum strain values recorded in the strain gauges (SG) at F_{max}, $\varepsilon_f^{F_{\max}}$, (see Table 4 and Fig. 12), where a decreasing trend between $\varepsilon_f^{F_{\max}}$ and ρ'_{fw} was obtained, justified by the detrimental interference of laminates. The largest strain value $\varepsilon_{f,\max}$ was recorded in L4S0, a specimen that did not have steel stirrups. Due to the interaction between existent steel stirrups and laminates, the strain level installed in the laminates tended to be lower as the percentage of stirrups increased. The relative position and inclination between stirrups and laminates might also affect the strain field installed in these reinforcements. Results of the next tests series will allow the influence of these variables to be quantified in terms of the internal forces shared by existent steel stirrups and applied CFRP laminates.

Table 4: Main obtained results

Specimen	ρ'_{fw}	F_{cr} (kN)	F_{max} (kN)	$\varepsilon_f^{F_{\max}}$ (‰)	$\varepsilon_{f,\max}$ (‰)
L0S0	-	570	751	-	-
L4S0	0.147	580	910	7.62 [2.58] *	11.15 [3.42] *
L1S3	0.037	490	923	8.23 [2.34] *	10.73 [3.96] *
L2S3	0.073	460	970	7.87 [2.70] *	7.95 [5.80] *
L7S3	0.257	550	1050	6.40 [2.55] *	7.17 [2.43] *

* [average vertical specimen strain]

From a comparison of the *F*-ε of L0S0 and L4S0 specimens, it can be concluded that laminates were very effective, not only in terms of specimen load carrying capacity, but also in stiffness after concrete cracking. Due to the resistance provided by the CFRP laminates crossing the cracks at F_{max}, the specimen horizontal strain decreased and the specimen vertical strain increased with the increase of ρ'_{fw}. Fig. 13 shows the evolution of the strains in the SG glued to the laminates (see also Fig. 8).

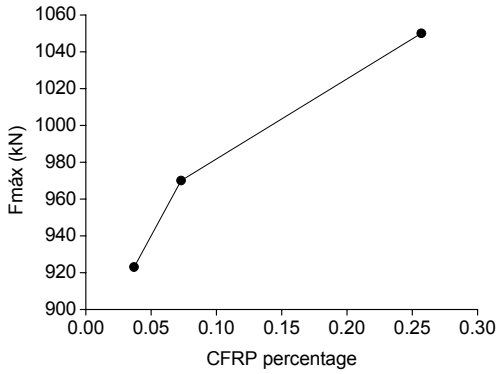

Figure 11: Maximum load vs CFRF strengthening ratio (ρ'_{fw})

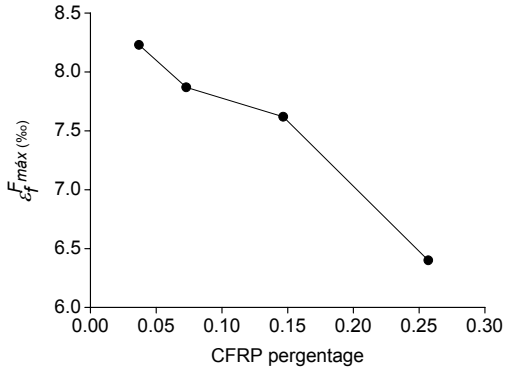

Figure 12: Maximum CFRP strain at F_{max} ($\varepsilon_f^{F_{\max}}$) versus CFRF strengthening ratio (ρ'_{fw})

It is concluded that the strains are marginal up to the formation of the main crack. As expected, the SG nearest to the loading plane presented the largest strain increment at the instant of crack formation, see Figure 13. However, during the loading procedure, the strains also increased significantly in the remaining SG. In the L4S0 and L1S3 specimens, the maximum strains exceeded 10 ‰. More significant is the fact that, after peak load (in the softening phase) the strains in the SGs more distant to the loading plane increased significantly, having attained a maximum value only slightly below the maximum strain value registered in the test. In L7S3, the maximum strain value in SG placed more distant to the loading plane did not exceed 2 ‰, which can be justified by the failure mode occurred in this specimen: the separation of the concrete layer that includes the laminates. The strain variation in the SGs of the L2S3 specimen was too distinct at the first phase after crack formation but, at peak load, the strains in the distinct SGs were almost similar.

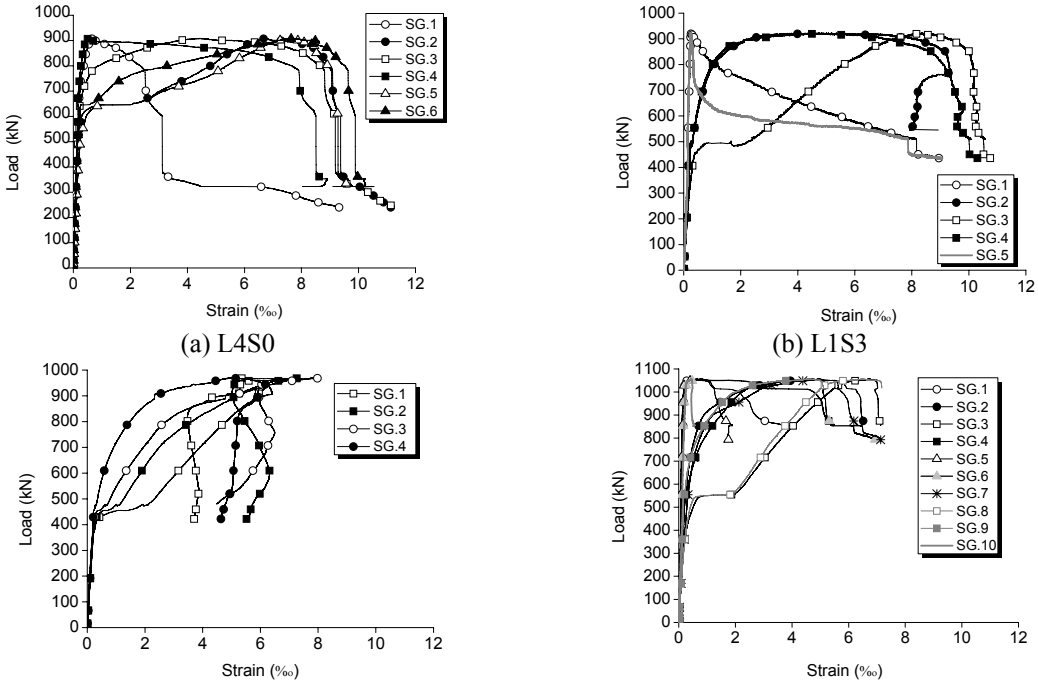

(a) L4S0 (b) L1S3

(c) L2S3 (d) L7S3

Figure 13: Strain variation on the laminates of: a) L4S0; c) L1S3; d) L2S3; e) L7S3

Fig. 14 represents the variation of the strains in the SG installed in the intermediate steel stirrup. As expected, the obtained results indicate that significant strains only occurred after cracking formation, especially at the SG nearest the loading plane. However, the maximum strain only exceeded $\varepsilon_{y0.2\%}$ in SG2 of L2S3 specimen, indicating that, for the geometrical arrangement of the stirrups and laminates considered in the present work, the laminates were more effective than stirrups in terms of supporting the applied load.

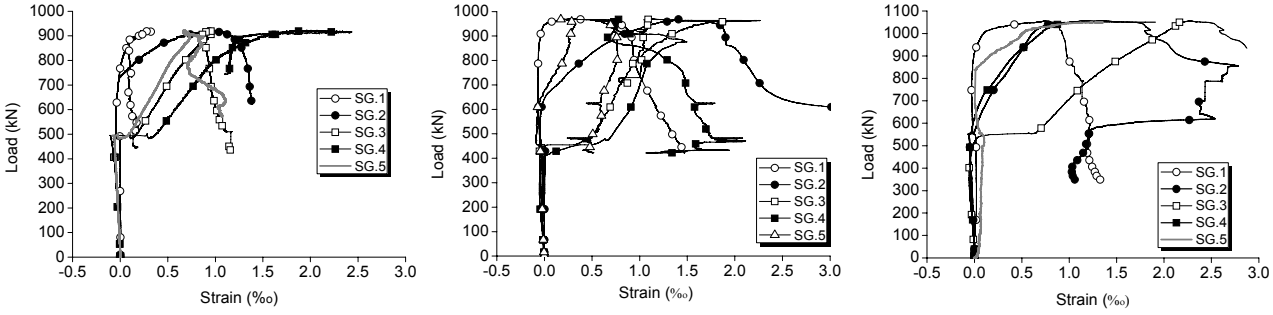

(a) (b) (c)

Figure 14: Strain variation on the steel stirrups of: a) L1S3; b) L2S3; c) L7S3

4 Conclusions

In the present work, a test set up was developed to assess the influence of the spacing and inclination of CFRP laminates installed according to the Near Surface Mounted technique for the shear strengthening of RC beams. This test set up can also evidence the influence between existent steel stirrups and applied CFRP laminates. From the results obtained in the carried out exploratory test series, the following main observations can be pointed out.

The CFRP laminates crossing a concrete failure crack were very effective in terms of load transference between both faces of the crack. However, this effectiveness decreased with the decreasing of the spacing between laminates, s_f. When s_f decreases, a detrimental effect between consecutive laminates occurs, which can be designated as "group effect", since below a certain s_f value a concrete layer that includes the laminates separates from the specimen concrete core. In consequence of this type of failure mode, the largest strain value recorded in the strain gauges installed on the laminates, at the specimen

maximum load, F_{max}, decreased with the decrease of s_f, which also justifies the loss of strengthening efficacy with the decrease of s_f. A post-test inspection of the failure modes of the laminates indicated that pure-debonding never occurred. In fact, a certain volume of concrete was fixed to the pulled-out length of the laminates, indicating that concrete tensile strength is a relevant parameter for the efficacy of NSM shear strengthening strategy. The observed tendency for the formation of a concrete conical surface at the pulled-out embedded length of the laminates provides extra information for the justification of the loss of strengthening efficacy when s_f decreases, since the available concrete fracture surfaces reduce with the decrease of s_f. However, even for the lowest s_f (50 mm), the maximum strain value at the laminates was still appreciable (about 7‰). Another interesting aspect is that, due to the sliding of the laminates, the maximum strain values in the laminates at the strain gauges (SG) positioned more distant to the critical crack were similar to the maximum values recorded in the SG nearest this crack.

From the analysis of the strain values in the laminates of specimens with and without internal steel stirrups, it seems that the strains in the laminates tend to be higher as the percentage of internal stirrups decreases. In fact, the maximum strain value in the laminates of specimen without internal stirrups (L4S0) was higher than the maximum strain value in the laminates of the specimen with internal stirrups and equivalent percentage of CFRP laminates (for this purpose the results of L2S3 and L7S3 specimens were considered).

Acknowledgments

The authors of the present work wish to acknowledge the support provided by the "Empreiteiros Casais", S&P®, Secil (Unibetão, Braga), degussa® Portugal and Civitest Companies. The study reported in this paper forms a part of the research program "CUTINSHEAR - Performance assessment of an innovative structural FRP strengthening technique using an integrated system based on optical fiber sensors" supported by FCT, POCTI/ECM/59033/2004. The second author acknowledges the post doctoral grant supported by the Portuguese Science and Technology Foundation (FCT).

References

[1] Barros, J.A.O.; Dias, S.J.E. 2006. Near surface mounted CFRP laminates for shear strengthening of concrete beams, *Journal Cement and Concrete Composites*, Vol. 28, No. 3, pp. 276-292.

[2] Dias, S.J.E.; Barros, J.A.O. 2006. NSM CFRP Laminates for the Shear Strengthening of T Section RC Beams, *2nd International fib Congress*, Naples, June 5-8, Paper 10-58 in CD.

[3] De Lorenzis, L., Rizzo, A. 2006. Behavior and capacity of RC beams strengthened in shear with NSM FRP reinforcement, *2nd International fib Congress*, Naples, June 5-8, Paper ID 10-9 in CD.

[4] Nanni A., Di Ludovico M., Parretti R., 2004. Shear strengthening of a PC bridge girder with NSM CFRP rectangular bars, *Advances in Structural Engineering*, Vol 7, No 4, pp. 97-109.

[5] Dias, S.J.E.; Barros, J.A.O. 2004. CFRP no reforço ao corte de vigas de BA: investigação experimental e modelos analíticos (CFRP for the shear strengthening of RC beams: Experimental and analytical research), Technical Report 04-DEC/E-08, Dep. Civil Eng., School of Eng., University of Minho, 108 p. (in Portuguese)

[6] American Concrete Institute, 2002, Guide for the Design and Construction of Externally Bonded FRP Systems for Strengthening Concrete Structures, *ACI 440.2R-02*, Farmington Hills, MI.

[7] Sena-Cruz J.M., and Barros J.A.O., 2004. Bond between near-surface mounted CFRP laminate strips and concrete in structural strengthening, *Journal of Composites for Construction*, vol. 8, No 6, pp. 519-527.

[8] CNR-DT200, 2004, Guidelines for design, execution and control of strengthening interventions by means of fibre reinforced composites, *National Research Council - advisory Committee on technical regulations for constructions*, CNR.

[9] Fib, 2001, Bulletin 14 - Externally Bonded FRP reinforcement for RC structures" Technical report, Task Group 9.3 FRP reinforcement for concrete structures.

[10] RILEM, 1994. *TC14–CPC, 1975: Modulus of elasticity of concrete in compression. Materials and Structures*, vol. 6, 30 p.

[11] EN 10 002–1, 1990. CEN: Metallic materials – Tensile testing. Part 1: Method of test (at ambient temperature), Bruxelas, 35 p.

[12] ISO 527-5, 1997, Plastics - Determination of tensile properties - Part 5: Test conditions for unidirectional fibre-reinforced plastic composites, International Organization for Standardization, Genève, Switzerland, pp 9.

[13] ISO 527-2, 1993, Plastics - Determination of tensile properties - Part 2: Test conditions for moulding and extrusion plastics, International Organization for Standardization (ISO), Geneva, Switzerland.

[14] Bonaldo, E.; Barros, J.A.O.; Lourenço, P.B. 2006. Strengthening technique combining CFRP laminates and compressive overlayer of steel fibre reinforced concrete to increase the flexural resistance of RC slabs, Technical report 06-DEC/E-05, Dep. Civil Eng., School Eng. University of Minho, 104 p.